Environmental Earth Sciences (2018) 77:297
https://doi.org/10.1007/s12665-018-7486-3

ORIGINAL ARTICLE

Mechanical and crack evolution characteristics of coal–rock under different fracture-hole conditions: a numerical study based on particle flow code

Xiao Wang[1,2] · **Long-gang Tian**[1,2]

Received: 7 October 2017 / Accepted: 7 April 2018 / Published online: 12 April 2018

Abstract
Coal–rock material contains many fractures and holes and it is of great significance to study their mechanical characteristics for understanding the instability mechanism of coal body. In this manuscript, considering fracture with different inclinations and hole with different positions, a variety of defective coal–rock specimens were established by PFC2D software, then characteristics of stress–strain and crack evolution law of coal–rock with different fracture-holes were discussed. The results show that mechanical properties, crack evolution characteristics, propagation forms of initial crack and final crack distribution form of coal–rock specimens with different fracture holes are different; the fracture angle has a larger influence than the hole position. Peak strength, peak strain, peak step and the total crack number show an increasing trend with the increase of fracture angle, while the crack initial propagation length becomes shorter and shorter.

Keywords Coal–rock · Fracture hole · Mechanics · Crack evolution

Introduction

With the increase of mine mining scale and development depth, rock burst, coal-gas outburst and other coal mine disasters are becoming more and more serious (He et al. 2005; Ning et al. 2018). Many researches showed that these disasters are closely related to the instability and failure of the coal–rock body (Mohamed et al. 2016; Wang et al. 2018). Natural coal–rock is composed of mineral particles and contains many defects, such as fractures and holes. These defects lead to the anisotropy of the coal–rock mass and the mechanical properties are very complex. Therefore, it is of great significance to study the mechanical characteristics of the defective coal–rock mass for understanding the instability mechanism of coal body.

✉ Xiao Wang
wangchxizo@163.com

✉ Long-gang Tian
lgtian@seu.edu.cn

[1] School of Civil Engineering, Southeast University, Nanjing 210096, China

[2] Institute of Future Underground Space, Southeast University, Nanjing 210096, China

In recent years, a lot of numerical calculations, laboratory tests and theoretical analyses have been done for the strength, deformation characteristics and crack evolution rules of defective rocks. As for fracture defects, Justo et al. (2010) using the rock mass classification systems estimated the modulus and strength of jointed rock; Bahaaddini et al. (2013) analyzed the effect of joint geometrical parameters on the mechanical properties of a non-persistent jointed rock mass by means of PFC3D software. Afolagboye et al. (2017) investigated the cracking behavior and coalescence process in a brittle material with two non-parallel overlapping fractures through high-speed camera. As for hole defects, Steen et al. (2005) carried out both experimental and numerical tests to analyze the damage pattern for a loaded disc with an eccentric hole. Li et al. (2015) discussed the dynamic compressive strength and crack propagation characteristics of prefabricated hole specimens. These researches play an active role in analyzing the instability mechanism of coal–rock body. However, there are few researches focusing on the combination flaws of fractures and holes. In this area, Yang and Huang (2014) carried out uniaxial compression tests on rectangular sandstone samples with two holes and one small fracture and the crack propagation characteristics were analyzed by means of particle flow software PFC.

In this manuscript, based on the above researches, the fracture-hole conditions are considered as one crack (40 mm in length and 2 mm in width) with seven different angles and one hole (the radius is 5 mm) at three different positions. The characteristics of stress–strain and crack evolution law of defective coal–rocks were discussed based on bonded particle model.

Numerical coal–rock models with different fracture-hole defects

Particle flow code (PFC)

Based on the discrete element method, Cundall and Strack (1979) established the particle flow (PFC) theory. PFC usually uses particles and bonds to characterize coal–rock materials. Among them, the discrete particles are represented by disks of unit thickness (PFC2D) or balls (PFC3D), which are considered rigid and have normal and tangential stiffness. There are two bonds that can be used to simulate the connection between coal–rock grains, named contact bond (CB) and parallel bond (PB) (Itasca consult group Inc. 2014). The CB model (Fig. 1a) has little resistance to the moment induced by particle rotation or shearing while PB model (Fig. 1b) can resist to such particle movements since PB model is acting like a beam that resists the bending moment occurring within the bonded area (Cho et al. 2007). When the bond is broken, the contact stiffness still active as long as the particle stay in contact. However, the bond stiffness will lose its effect regardless of whether particles stay in contact or not. In this study, the uniaxial compression model for defective coal–rock specimens was built using the parallel bond.

Parameter checking of coal–rock

Microscopic physico-mechanical parameters of the particles and the bond properties are required for running the simulation tests using the particle flow theory. However, these parameters cannot be directly acquired from laboratory tests (Wang et al. 2016). Therefore, the microscopic parameters selection and verification were needed before the numerical simulation. During this process, a large number of numerical simulation tests with similar conditions as the laboratory tests or in situ field tests were first carried out. Then, the numerical simulation results were compared against the results of laboratory tests or in situ field tests. The microscopic parameters were adjusted repeatedly by "trial and error" method (Castro-Filgueira et al. 2017) until they satisfied the requirement of simulation analysis. The "trial and error" method parameter

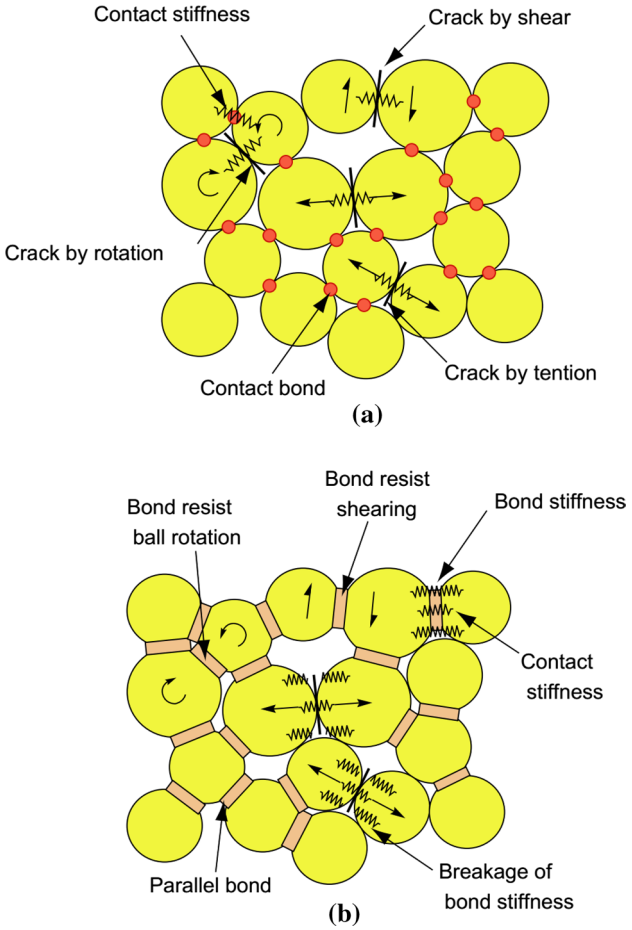

Fig. 1 Cohesive model and its micro-mechanical behavior schematic diagram (Cho et al. 2007). **a** Contact bond model. **b** Parallel bond model

checking process of PFC model (version 5.0) is shown in Fig. 2. The parameter of m_i is the Hoek–Brown strength parameter.

Owing to the limitation of laboratory test condition, the parameters provided by Wang et al. (2016) were used to carry out numerical test. In his manuscript, the mechanical parameters of uniaxial compression of standard coal–rock specimens in a certain mining area were selected as the reference basis for the particle flow program. The size of the numerical model is 50 mm (length) × 100 mm (height) and the loading rate is 0.02 mm/s (the same as the experimental test used). Through the method of "trial and error" with repeated check comparison, the physical mechanical parameters of Table 1 were close to the macroscopic mechanical parameters of the real coal–rock mass. The stress–strain curve (Fig. 3) and the final failure characteristics (Fig. 4) of PFC model under uniaxial compression are in good agreement with the laboratory tests of real coal–rock.

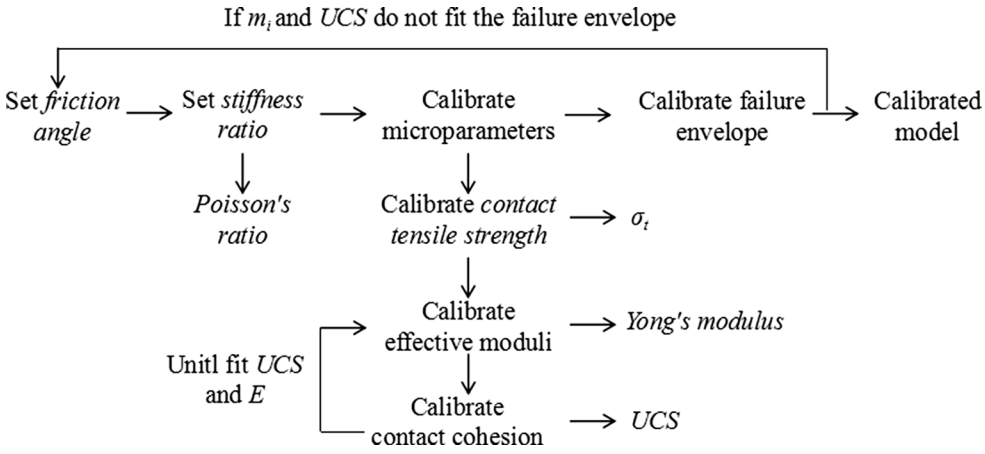

Fig. 2 The "trial and error" method parameter checking process of PFC model (Castro-Filgueira et al. 2017)

Table 1 Physico-mechanical parameters of coal–rock specimen (Wang et al. 2016)

Parameter	Value	Parameter	Value
Minimum particle diameter (mm)	0.3	Porosity	0.1
Particle diameter ratio	1.66	Coefficient of friction	0.46
Density (kg/m^3)	1800	Parallel bond compressive strength (MPa)	10
Contact modulus of the particle (GPa)	1.0	Parallel bond friction angle (°)	25
Parallel bond deformation modulus (GPa)	12	Parallel bond cohesive force (MPa)	16
Contact bond gap (mm)	0.05	Stiffness ratio	1.0
Normal critical damping ratio	0.5		

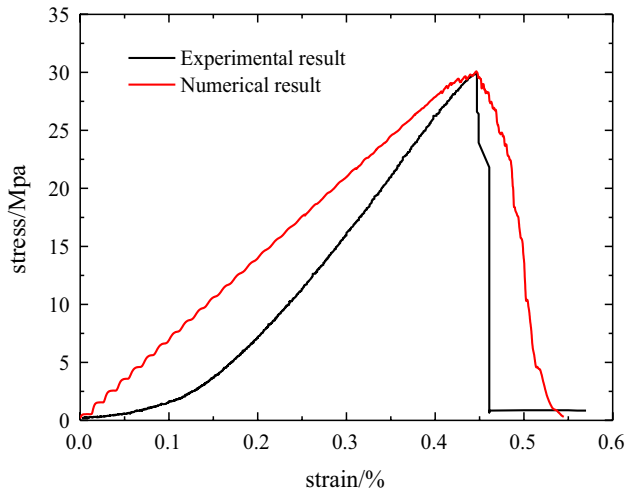

Fig. 3 The comparison between the numerical and experimental stress–strain curves of intact coal–rock specimens (Wang et al. 2016)

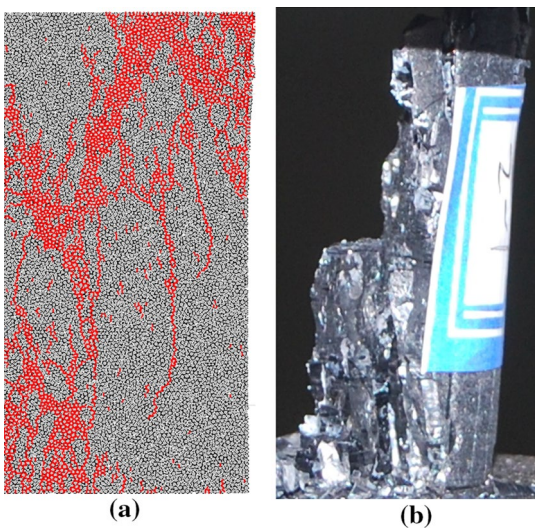

Fig. 4 Failure modes of intact coal–rock specimens obtained through simulation and experiment (Wang et al. 2016). **a** Numerical result **b** experimental result

Numerical models of coal–rocks with different fracture-hole defects

To study the mechanical characteristics and crack evolution law of defective coal–rock mass, 21 different coal–rock models with different fracture-hole defects were built (Fig. 5). These models were first established as intact coal–rock based on the parameters of Table 1, then fracture-holes were installed before running the tests. There were seven kinds of fracture angles (0°, 15°, 30°, 45°, 60°, 75°, 90°, respectively) and they all went through the original point (0, 0). The holes were arranged with

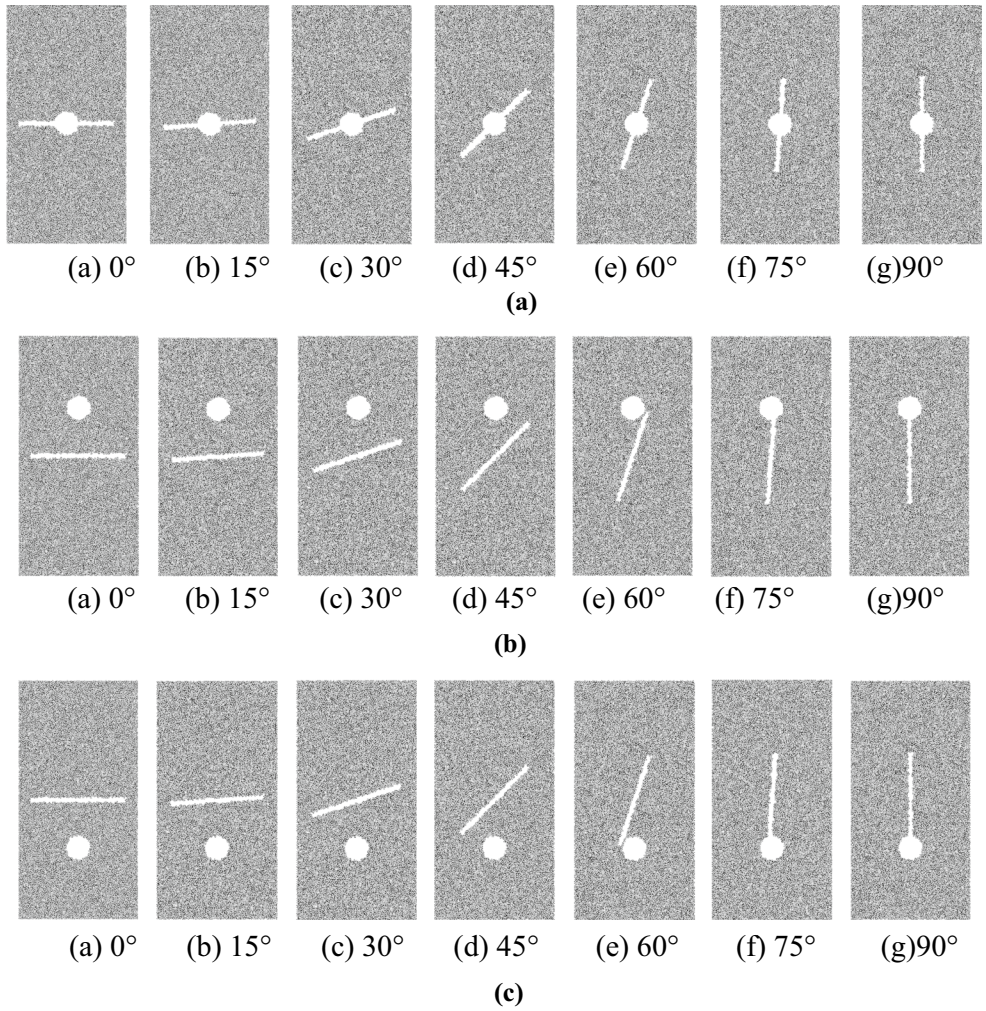

Fig. 5 Numerical coal–rock specimens with different fracture-hole defects. **a** Group 1: the coal–rock specimens whose defective hole center was at the original point, **b** Group 2: the coal–rock specimens whose defective hole center was 20 mm above the original point, **c** Group 3: the coal–rock specimens whose defective hole center was 20 mm below the original point

three schemes: located at the original point, located 20 mm above original point, and located 20 mm below the original point. The radius of the holes was 5 mm and the size of the fractures was 40 mm (length) × 2 mm (width). To facilitate the analysis, these 21 defective coal–rock specimens were divided into 3 groups according to the hole position. As shown in Fig. 5, the first group was the coal–rock specimens whose defective hole center was at the original point. In the second group, defective hole center was 20 mm above the original point and in the third group, defective hole center was 20 mm below the original point. Load was controlled by applying compress displacement at top of the specimen, with the rate of 0.02 mm/s. The numerical test ends when residual stress of the specimens reached 1% of its peak strength by controlling the FISH language.

Test results analysis

Properties of strength and deformation

Figure 6 shows the stress–strain curves of coal–rock specimens with different fracture-hole defects and Table 2 lists the measured concrete values of peak strength and peak strain.

The mechanical properties of coal–rock specimens with different fracture-holes are different. When the hole is located at a fixed place, the uniaxial compressive strength of coal–rock shows an increasing trend along with the increase of the fracture angle and the stress–strain curve can be divided into three types according to the fracture angle. The first type has two peaks, one small peak and followed by a

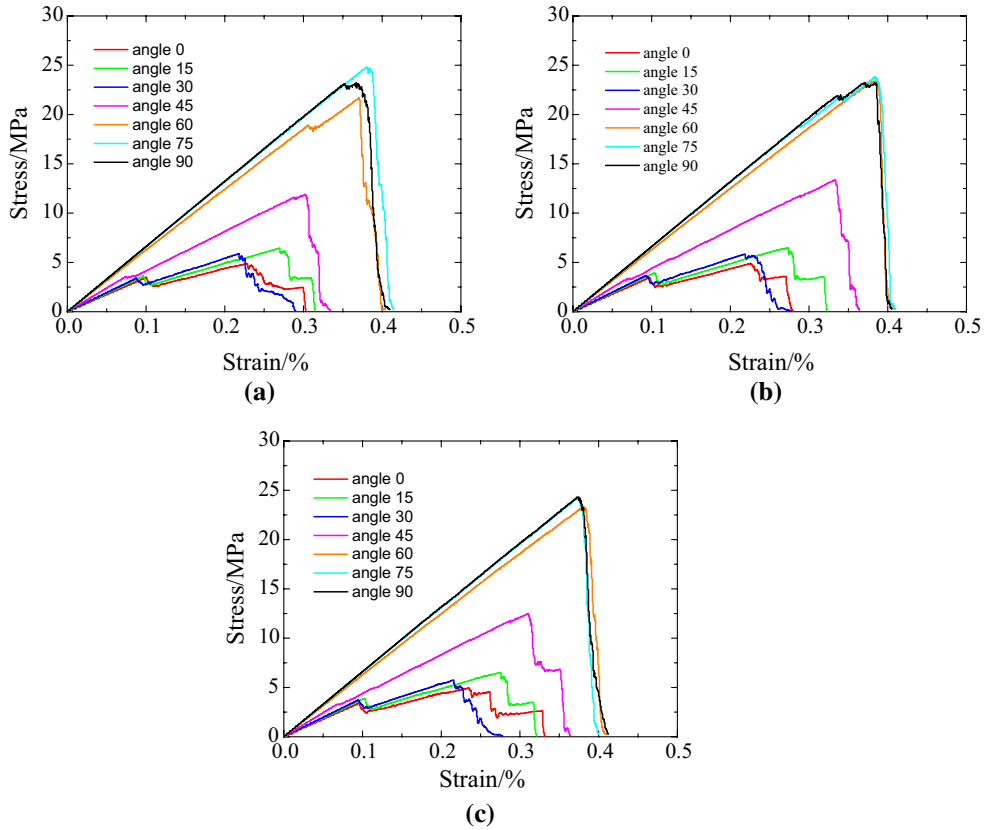

Fig. 6 Stress–strain curves of coal–rock specimens with different fracture-hole defects. **a** Group 1 **b** Group 2 **c** Group 3

Table 2 Peak strength and peak strain of different defective coal–rock specimens

Fracture angles (°)	Peak strength (MPa)			Peak strain (%)		
	Group 1	Group 2	Group 3	Group 1	Group 2	Group 3
0	4.888	4.903	4.966	0.229	0.226	0.235
15	6.464	6.470	6.512	0.270	0.273	0.275
30	5.867	5.844	5.730	0.218	0.219	0.215
45	11.869	13.400	12.502	0.303	0.333	0.310
60	21.696	23.376	23.344	0.371	0.386	0.381
75	24.812	23.842	24.300	0.380	0.385	0.374
90	23.166	23.248	24.329	0.367	0.385	0.373

large peak; the post-peak stress curve is not smooth, with a certain force retention phase; the peak strength, peak strain and elastic modulus are at a lower level relatively when compared with the others. This type includes the defective coal–rock specimens with fracture angle of 0°, 15° and 30°, for example, the stress–strain curve of the coal–rock specimen with fracture angle of 15° and the hole located at the original point (Fig. 6a Group 1). The stress increase with the increase of the strain reaches its first peak (3.4 MPa) when the strain is about 0.1%, then the stress drops down to about 2.8 MPa. After this valley, the stress increases again and reaches its second peak (about 4.9 MPa) when the strain is about 2.3%. Then, the stress falls down to about 3.4 MPa and the value remains (about 0.017% strain value) before drops to the lowest value. The second type includes the defective coal–rock specimen with fracture angle of 45°. The feature is that peak strength (about 12.5 MPa), peak strain (about 0.33%) and elastic modulus (about 4.02 GPa) are in the middle range. The third type shows a higher peak strength (about 23.6 MPa), peak strain (about 0.38%) and elastic modulus (about 6.42 GPa) and the stress drops down rapidly after the peak. The stress–strain curves of coal–rock models with fracture angle of 60°, 75° and 90° can be classified as this type.

When the fracture angle is constant, the change of peak strength, peak strain and elastic modulus of the defective specimens are very little with the change of the hole position. For example, when fracture angle is 45°, the peak strengths of the defective coal–rock specimens with the hole located at the original point, 20 mm above the original point and 20 mm below the original point are 11.9, 13.4 and 12.5 MPa, and the gap between them is less than 1.5 MPa; the peak strains are 0.30, 0.33, 0.31% and the gap between them is less than 0.03%; the elastic moduli are 4.03, 3.97, 4.02 GPa and the gap between them is less than 0.06 GPa.

Laws of crack evolution

The relation curves between the numerical step and the crack number of different fracture-hole defective coal–rock specimens are shown in Fig. 7 and the measured concrete values of peak step and peak crack number are listed in Table 3.

In the process of defective coal–rock specimens compression, the crack evolution also can be divided into three stages. The first stage is zero crack stage, the second stage is crack slowly propagating stage, and the third stage is the crack rapid growth stage. In the first stage, the coal–rock specimens do not produce any cracks because there is no parallel bond failure. This phenomenon does not agree with the real coal–rock mass test, for which may produce

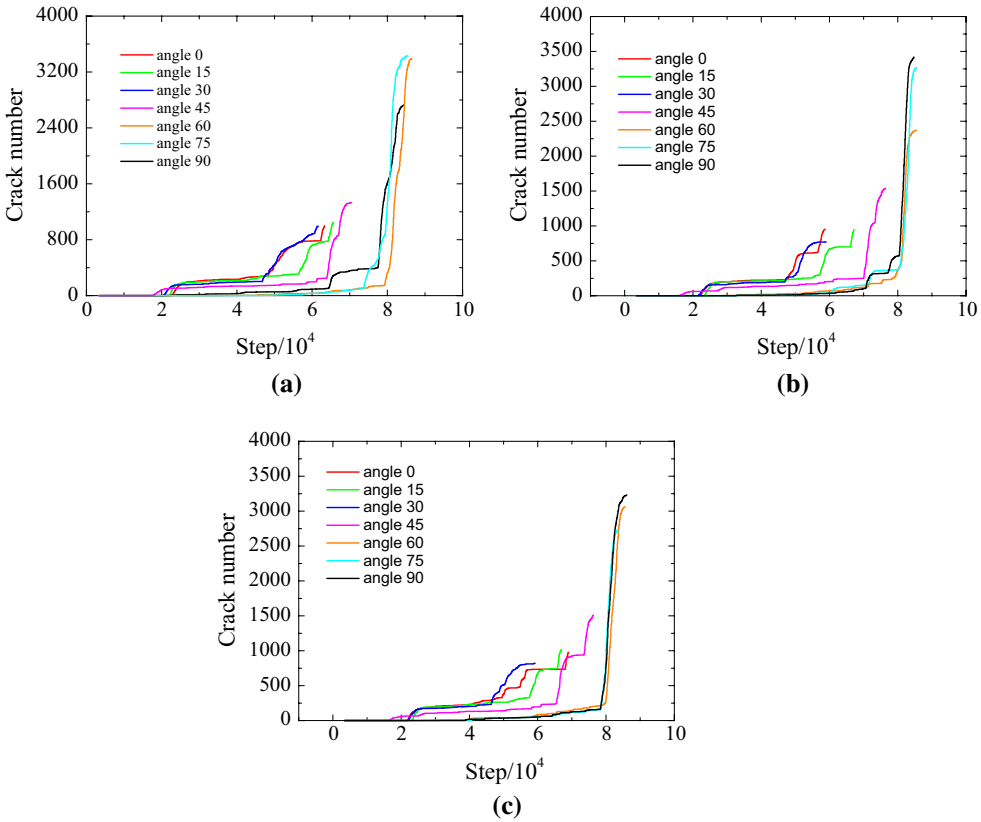

Fig. 7 Relation curves between the numerical step and the crack number of different fracture-hole defective coal–rock specimens. **a** Group 1 **b** Group 2 **c** Group 3

Table 3 Peak step and peak crack number of different defective coal–rock specimens

Fracture angles (°)	Peak step			Peak crack number		
	Group 1	Group 2	Group 3	Group 1	Group 2	Group 3
0	48,580	48,050	49,820	328	274	368
15	56,750	57,460	57,830	354	346	376
30	47,070	47,290	46,530	253	246	267
45	64,090	70,240	65,600	313	353	303
60	77,710	80,750	79,780	493	438	252
75	79,690	80,620	78,480	263	421	178
90	76,960	80,590	78,270	473	672	161

some cracks due to the closure of the initial fracture. In the second stage, the coal–rock specimen will produce cracks continuously, but the crack number is not large. As for the third stage, cracks continue to develop and the rate of crack growth is quite large.

Different fracture-hole combinations of coal–rock specimens have different characteristics of crack evolution. When the position of the hole is fixed, the total crack number of coal–rock shows an increasing trend along with the increase of the fracture angle and the crack evolution curve can also be divided into three types according to the fracture angle. The division method is the same as that of the stress–strain curve, the first type includes fracture angle of 0°, 15°, 30°, the second type includes fracture angle of 45° and the third type includes fracture angle of 60°, 75°, 90°. For the first type, crack number is larger than the others during the crack slowly propagating stage and in the crack rapid growth stage; they are relatively gentle and accompanied by some gentle fluctuations. Meanwhile, time required to reach the peak strength is the fewest, just about 49,000 steps. For the second type, the crack number is in the middle level during crack slowly propagating stage and crack rapid growth stage. The time to reach the peak is about 66,000 steps and it is in the middle level when compared with the others. While the third type crack evolution curve, the crack number is the smallest during the crack slowly propagating stage and the largest during the crack rapid growth stage. In addition, the needed time to reach the peak strength is the largest, about 80,000 steps.

However, there are no recognizable features for the crack number at the peak strength moment. For example, from 0° to 90°, the crack number of Group 1 at the peak strength moment is 328, 354, 253, 313, 493, 263 and the crack number of Group 3 at the peak strength moment is 368, 376, 267, 303, 252, 178. The evolution trend of the crack number at the peak strength moment of Group 1 is increase, decrease, increase, and decrease with the increase of the fracture angle, while the evolution trend of Group 3 is decrease, increase, and decrease.

When the fracture angle is confined in a degree, the crack evolution characteristics of defective coal–rock specimens similarly vary with the hole position, but they also show some discrete features. For example, when the fracture angle is confined in 45°, crack evolution feature differs from the others during the crack slow development stage and when the fracture angle is confined in 90°, the total crack number and final steps are much smaller than the others.

Characteristics of failure mode

It can be seen from the propagation forms of initial crack of different defective coal rocks in Fig. 8 that when the hole is located at a fixed place, the initiation length of the crack becomes shorter and shorter with the increase of fracture angle. The propagation forms of initial crack show three different types: for type one, cracks propagation from holes and fractures; for type two, cracks propagation from holes and for type three, cracks propagation from fractures. As for Group 1, along with the increase of the fracture angle, the propagation forms of initial crack of coal–rock specimens include all these three types (angle degrees of 0, 30 corresponding to type one, 15 corresponding to type two and 45, 60, 75, 90 corresponding to type three); while for Group 2 and Group 3, the propagation forms of initial crack are just type one. Meanwhile, the initial propagate length of the cracks becomes more and more short as the increase of the fracture angle. When the fracture angle is constant, the initial crack length varies little with the hole position, but the propagation forms of initial crack have obvious differences. As the fracture angle is 15°, the propagation forms of initial crack are type two when the hole in the original point and the propagation forms of initial crack is type one when the hole above or below 20 mm of the original point.

Figure 9 shows the final crack distribution forms of these 21 defective coal–rock numerical models. When the position of the hole is fixed, the crack amount increases with the increase of the fracture angle and there are three kinds of the final crack distribution forms. For the first type, most cracks distribute at both ends of the fracture; for the second type, most cracks distribute at the end of the fracture and the periphery of the hole and for the third type, most cracks distribute only around the hole. In addition, with the increase of the fracture angle, deformation of the fracture and the hole is larger and larger. When the fracture angle is confined in a degree, the crack density varies little with the hole position, but the final crack distribution forms are quite different. Under the combined effect of the fracture and hole, the failure modes of coal–rock mass are various, which explains the irregular evolution of stress at the post-peak stage. In practical engineering, the failure modes of coal–rock mass can be controlled by prefabricating fractures and holes in coal–rock mass according to these damage laws of defective coal–rock specimens.

Conclusions

In this manuscript, the mechanical behavior and crack evolution law of coal–rock with different fracture-holes were studied by numerical tests and the following conclusions could be drawn.

The mechanical properties, crack evolution characteristics, propagation forms of initial crack and crack final distribution form of different defective coal–rock specimens are different. When the position of the hole is fixed, the peak strength, peak strain, peak step and the total crack

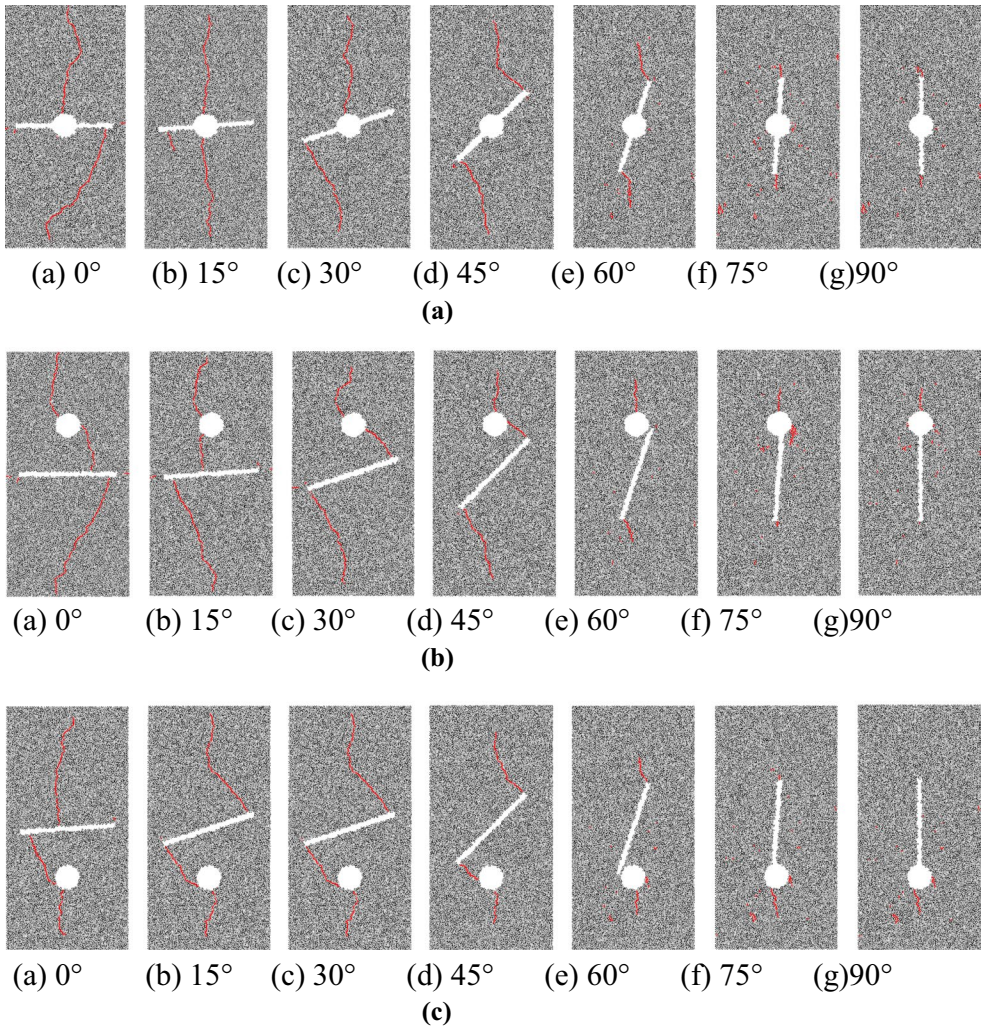

Fig. 8 Propagation forms of initial crack of coal–rock specimens with different fracture-hole defects. **a** Group 1 **b** Group 2 **c** Group 3

number show an increasing trend with the increase of the fracture angle, but the initial propagation length of the crack becomes shorter and shorter. When the fracture angle is constant, these parameters vary little with the change of the hole position.

The stress–strain and crack evolution curves can be divided into three different types according to the fracture angle. The first type includes the fracture angles of 0°, 15° and 30°, the second type includes the fracture angle of 45° and the third type includes the fracture angles of 60°, 75° and 90°. In addition, during the progress of the tests, the crack evolution curve has three stages, the zero crack stage, the crack slowly propagating stage, and the crack rapid growth stage.

With the change of the combination form of fractures and holes, the failure mode of these defective coal rocks is different, but they also have some common characteristics. When the hole is located at a fixed place, the initial propagation length of the crack becomes shorter and the final crack number becomes larger along with the increase of fracture angle. The propagation forms of initial crack have three types: for type one, cracks propagation from holes and fractures; for type two, cracks propagation from holes and for type three, cracks propagation from fractures. The final crack distribution form also have three types: for the first type, most cracks distribute at both ends of the fracture; for the second type, most cracks distribute at the end of the fracture and the periphery of the hole and for the third type, most cracks distribute only around the hole.

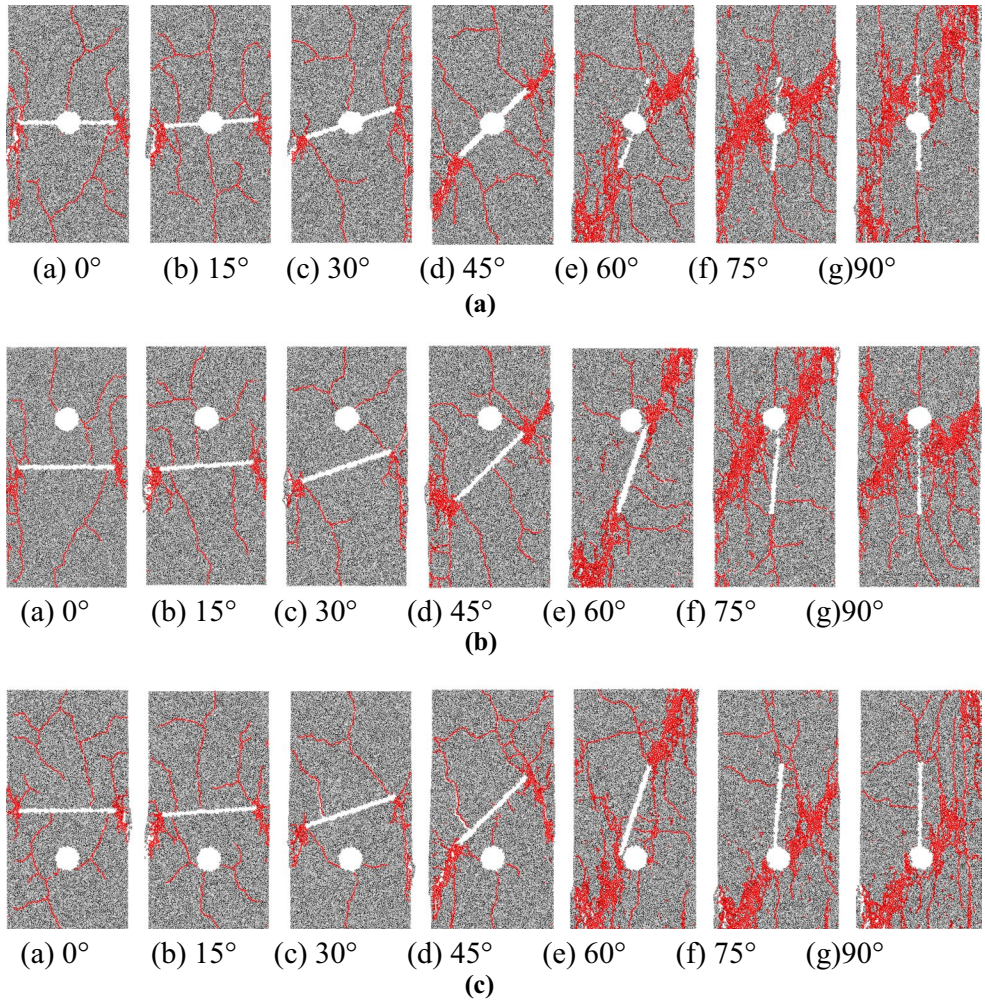

Fig. 9 Final crack distribution forms of different fracture-hole defective coal–rock specimens. **a** Group 1 **b** Group 2 **c** Group 3

Acknowledgements The authors would like to acknowledge the support of the Natural Science Foundation of Jiangsu Province (No. BK20170670), the Fundamental Research Funds for the Central Universities (No. 3205007810), and the National Natural Science Foundation of China (No. 51304126, 51704179).

References

Afolagboye LO, He J, Wang S (2017) Experimental study on cracking behaviour of moulded gypsum containing two non-parallel overlapping flaws under uniaxial compression. Acta Mech Sin 33(2):394–405. https://doi.org/10.1007/s10409-016-0624-9

Bahaaddini M, Sharrock G, Hebblewhite BK (2013) Numerical investigation of the effect of joint geometrical parameters on the mechanical properties of a non-persistent jointed rock mass under uniaxial compression. Comput Geotech 49:206–225. https://doi.org/10.1016/j.compgeo.2012.10.012

Castro-Filgueira U, Alejano LR, Arzúa J et al (2017) Sensitivity analysis of the micro-parameters used in a PFC analysis towards the mechanical properties of rocks. Proc Eng 191:488–495. https://doi.org/10.1016/j.proeng.2017.05.208

Cho N, Martin CD, Sego DC (2007) A clumped particle model for rock. Int J Rock Mech Min Sci 44(7):997–1010. https://doi.org/10.1016/j.ijrmms.2007.02.002

Cundall PA, Strack OD (1979) A discrete numerical model for granular assemblies. Geotechnique 29(1):47–65. https://doi.org/10.1680/geot.1979.29.1.47

He MC, Xie HP, Peng SP et al (2005) Study on rock mechanics in deep mining engineering. Chin J Rock Mech Eng 24(16):2803–2813 **(in Chinese)**

Itasca Consulting Group Inc. (2014) PFC (particle flow code), version 5.0. ICG, Minneapolis

Justo JL, Justo E, Azañón JM et al (2010) The use of rock mass classification systems to estimate the modulus and strength of jointed rock. Rock Mech Rock Eng 43(3):287–304. https://doi.org/10.1007/s00603-009-0040-6

Li D, Cheng T, Zhou T et al (2015) Experimental study of the dynamic strength and fracturing characteristics of marble specimens with a single hole under impact loading. Chin J Rock Mech Eng 34(2):249–260 **(in Chinese)**

Mohamed KM, Murphy MM, Lawson HE et al (2016) Analysis of the current rib support practices and techniques in U.S. coal mines. Int J Min Sci Technol 26(1):77–87. https://doi.org/10.1016/j.ijmst.2015.11.014

Ning JG, Wang J, Jiang JQ et al (2018) Estimation of crack initiation and propagation thresholds of confined brittle coal specimens based on energy dissipation theory. Rock Mech Rock Eng 51(1):119–134. https://doi.org/10.1007/s00603-017-1317-9

Steen BVD, Vervoort A, Napier JAL (2005) Observed and simulated fracture pattern in diametrically loaded discs of rock material. Int J Fract 131(1):35–52. https://doi.org/10.1007/s10704-004-3177-z

Wang X, Wen ZJ, Jiang YJ (2016) Time-space effect of stress field and damage evolution law of compressed coal-rock. Geotech Geol Eng 34(6):1933–1940. https://doi.org/10.1007/s10706-016-0074-y

Wang X, Wen ZJ, Jiang YJ et al (2018) Experimental study on mechanical and acoustic emission characteristics of rock-like material under non-uniformly distributed loads. Rock Mech Rock Eng 51(3):729–745. https://doi.org/10.1007/s00603-017-1363-3

Yang SQ, Huang YH (2014) Experimental and particle flow simulation on crack coalescence behavior of sandstone specimens containing double holes and a single fissure. J Basic Sci Eng 22(3):584–596 **(in Chinese)**